

YOUNG'S MODULUS PREDICTION OF LONG FIBER REINFORCED THERMOPLASTICS

F. Garesci^a, S. Fliegner^b

Corresponding author: F. Garesci: fgaresci@unime.it

*a) DIECII – Department of Electronic Engineering, Industrial Chemistry and Engineering,
con.da di Dio – University of Messina, Italy*

b) Fraunhofer Institute for Mechanics of Materials IWM, Freiburg, Germany

Keywords:A. Glass fibres B. Mechanical properties. C. Elastic properties

Abstract

The aim of this paper is to provide analytical models able to predict the elastic properties of long fiber reinforced thermoplastics (LFT) in dependence of microstructural parameters such as the fiber volume content (v_f), the fiber orientation distribution (FOD) and the fiber length distribution (FLD). The analytical predictions are compared to the experimental stiffness values from tensile tests on the composite materials showing a good agreement. The FLD in terms of the probability density distribution as function of the fiber aspect ratio has been computed by an automated fiber separation and image analysis tool. On the other hand, the FOD in terms of the probability density distribution as function of fiber in-plane orientation was identified by using an image correlation procedure based on computer tomography scans of characteristic LFT specimens. Our analysis shows a good performance to predict the Young's Modulus of LFT due to incorporation of the FOD as well as the FLD into the calculations.

Introduction

In the last years, the demand of high performing and economically producible materials for automotive applications is growing. LFT are a promising solution meeting the criteria cited

above, in particular they provide a good specific stiffness and strength if the part design is adapted to the respective load cases. The efficient value of the material properties such as elastic stiffness and strength varies in a broad range up to 250% [18], [19]. Those values depend on the process-driven microstructural properties such as the fiber volume content (v_f), the fiber orientation distribution (FOD) and the fiber length distribution (FLD) and they must be considered in order to fully exploit the lightweight potential of LFT. In this work, the elastic stiffness of LFT is derived from the characteristic values of the microstructure by means of analytical models. There are several procedures in literature for predicting the properties of composite materials in dependence of their microstructure. Tucker et al. [1] provide a good overview on the micromechanical models used to calculate the stiffness of short fiber composites. This traditional approach combines several methods such as the Eshelby equivalent inclusion, the Mori-Tanaka models and the Halpin-Tsai equations [2] to predict the elastic properties of short fiber reinforced plastics in dependence of both fiber orientation and volume content. Other authors [3], [4], [5] use a unidirectional short fiber composite and improve the micromechanical models by taking into account the spatial distribution of the reinforced fibers. In this way, it is also possible to predict the local thermo-mechanical properties excellently. Other studies focus on the closure approximations [6],[7], [8] for evaluating the thermoelastic properties of short fiber composite to optimize the injection moulding process. A recent study [9] is based on the elastic prediction of the correct experimental fiber length distribution (FLD) and the correct fiber orientation distribution (FOD). The fiber dimension could be a relevant aspect for understating the elastic properties of composites. Simple models are based on the prediction of spherical particles [12] or short fiber composite, but recently studies focused on not aligned long fiber composite [13] and classic theory applied to new materials like carbon nanotubes [14] and nano composite [15] are very promising in term of understating the elastic properties. Other authors focused their

methodology in the effect of the interfacial bonding conditions only to evaluate the effective properties of the composite [10], [11]; while others used finite element method in order to investigate how two of the most widespread models (i.e. Tandon-Weng and Halpin-Tsai) are suitable to predict either the stiffness of short fiber composite [21] and a composite by applying the orientation averaging scheme (several hundred multi-fiber with different orientation states [22]). In Ref. 12 the two previous approaches are modified in two relevant steps. Firstly, by incorporating an experimental FLD as well as a fiber orientation distribution (FOD) and secondly by evaluating the Mori-Tanaka model to obtain the stiffness matrix of the aligned fiber composite containing the previous FLD.

In this article, the elastic stiffness of a commercial long fiber reinforced thermoplastic has been investigated by using a hybrid procedure based on a theoretical approach describing the transversely isotropic equivalent composite. The model uses the experimental data of the fiber orientation and length distributions. To validate the procedure the predicted stiffness values are compared with experimental values from tensile tests. The scenario of the experimental framework presented in this manuscript is different from the works that studied short fiber composite (aspect ratio near the value of 20); in fact, in our experimental data the smallest value measured of aspect ratio is 27. In addition, if we considered the long fiber studies, most of them don't use directly experimental FLD but the corrected FLD data or the Monte Carlo method. The advantage of our procedure is due to the direct use of the experimental data and thus to predict the stiffness properties of LFT rather quickly. The working scheme is given by three main steps:

1. Experimental methods and materials:

- 1.1. Tensile tests to determine the elastic stiffness of the LFT material;
- 1.2. Microstructure analysis by means of computer tomography to analyse the Fiber Orientation Distribution (FOD)

1.3. Automated fiber separation and analysis procedure to investigate the Fiber Length Distribution (FLD)

2. Analytical Procedure:

2.1. Halpin-Tsai theory to evaluate the properties of the transversely isotropic composite;

2.2. Fiber Orientation Distribution function to determine the tensor rank2 a_{ij} and the tensor rank4 a_{ijkl} after Advani, Tucker [16];

2.3. Mean Tensor Averaging procedure to predict the Elastic Properties of LFT.

3. Fit functions:

3.1. Curve Fitting Procedure for Fiber Orientation Distribution(FOD);

3.2. Curve Fitting Procedure for Fiber Length Distribution (FLD).

1. EXPERIMENTAL METHODS AND MATERIALS

The LFT material was produced by a so-called direct LFT production route, where the continuous fiber roving are introduced directly into a double screw extruder and are broken into fiber fragments by the overlapping edges of the contra-rotating screws. The resulting material is characterized through a broad FLD reaching from a large amount of fiber fragments well below 1 mm until very long fibers up to 50 mm. The matrix consists of polypropylene resin (DOW® C711-70RNA) with some stabilizers and coupling agents and is merged with 30 mass-% glass fibers (TufRov® 4575) to form the LFT composite. To simulate different material states in terms of a locally varying microstructure, 3 mm thick plates with outer dimensions of 400 x 400 mm were produced by compression molding. The LFT-D strand as it comes out of the extruder was placed asymmetrically in the mold to separate the so-called press region near the strand inlay position from the flow-region, where a lateral flow is responsible for a higher degree of fiber orientation compared to the press-region.

1.1. Tensile tests to determine the elastic stiffness of the LFT material

The tensile stiffness of specimens with different orientation relative to the fiber mean orientation or flow direction, but similar fiber volume fraction and fiber length distribution was determined with a Hegewald&Peschke “Inspekt 100” testing machine. The specimen geometry was chosen according to DIN EN ISO 3167. The tests were performed at a strain rate of approximately 0.00022 [mm/s] to a maximum stress of 10 MPa in order avoid any damage. Three loading-unloading cycles per specimen were performed. The stiffness is taken as the mean value of the three loading cycles. At least three specimens per orientation were tested. The stiffness values for E_{11} and E_{22} are 7.83 and 3.25 GPa and 6.49 and 3.77 GPa for flow and press region LFT (30 mass-% / 13 volume-% fiber fraction) respectively.

1.2. Microstructure analysis by means of computer tomography

Microstructure analysis has been performed on specimens from different regions of a 3 mm thick LFT-plate. Because of the thin cross section, the fibers are aligned in planes parallel to the specimen surface and the out-of-plane component of the fiber orientation is negligibly small. The specimens for computer tomographic analysis have been prepared from similar regions as the specimens for mechanical testing were taken from. The tomography scans have been performed on a Phoenix “nanome|x 180NF” with a voxel size of 5 - 8 μm , so the complete plate thickness could be analyzed with one scan. The data was analyzed by the plug in “Directionality” for ImageJ [20], after converting the 3D voxel data to a stack of 2D images parallel to the surface. The 2D images parallel to the surface 2D orientation histograms have been extracted for each of the stack. The resulting orientation distribution for the whole stack has been generated by summing up the single histograms and re-normalizing.

Flow region specimens (figure 1.a) were taken from a region of approx. 100 mm distance from the LFT strand inlay position, so a relatively high amount of fiber alignment results from the lateral flow field inside the mold. A low degree of fiber waviness can be observed in a characteristic CT scan of a flow region specimen. However, the scan shows only a section of

approx. 2.8 mm edge length due to resolution limits of the scanning device. An exemplary CT scan of a press region specimen (figure 1.b) exhibits remarkable deviation from the flow region structure which can be explained by a different flow field during specimen fabrication and thus a significantly lower degree of fiber alignment.

1.3. Automated fiber separation and analysis procedure

The FLD was determined with a characteristic LFT specimen of a size of approx 70x40x3 mm³. The specimen was first incinerated and then dispersed in a dilute solvent to separate the fibers. Finally, the fibers were analyzed by the image analysis software “FASEP®”. The procedure was carried out by the company “xyz high precision” [17].

2. ANALYTICAL PROCEDURE

2.1. Halpin-Tsai theory to evaluate the properties of the transversely isotropic composite

The Halpin Tsai equations are used to predict the mechanical properties of continuous long fiber composites [2]:

$$\frac{P_c}{P_m} = \frac{1 + \zeta \eta V_f}{1 - \eta V_f} \quad (1)$$

where P_c and P_m are the composite properties (E_{11}, E_{22}, G_{12}) and the matrix properties respectively, ζ is a measure of reinforcement geometry and loading conditions and η is a fiber parameter computed as:

$$\eta = \frac{P_f / P_m - 1}{P_f / P_m + \zeta} \quad (2)$$

For continuous, cylindrical fiber reinforced composites the geometry factor is given as:

$$\begin{aligned} \zeta_{E11} &= 2 \cdot AR + 40V_f^{10} \\ \zeta_{E22} &= 2 + 40V_f^{10} \\ \zeta_{G12} &= 1 + 40V_f^{10} \end{aligned} \quad (3)$$

If the fibers are aligned along 1-direction and the behaviours in the 2-direction and 3-direction are identical, the composite can be treated as transversely isotropic. Under this hypothesis the following identities hold: $E_{22} = E_{33}$, $\nu_{12} = \nu_{13}$, $G_{12} = G_{13}$ and the following relationship is verified:

$$G_{23} = E_{22}/2(1 + \nu_{23}) \quad (4)$$

In this scenario, the independent constants for the transversely isotropic material are only five

(i. e. $E_{11}, E_{22}, G_{12}, \nu_{12}, \nu_{23}$) and the Compliance Matrix [S] can be expressed by:

$$[S] = \begin{bmatrix} 1/E_{11} & \nu_{21}/E_{22} & -\nu_{31}/E_{33} & 0 & 0 & 0 \\ -\nu_{12}/E_{11} & 1/E_{22} & -\nu_{32}/E_{33} & 0 & 0 & 0 \\ -\nu_{13}/E_{11} & -\nu_{23}/E_{22} & 1/E_{33} & 0 & 0 & 0 \\ 0 & 0 & 0 & 1/G_{23} & 0 & 0 \\ 0 & 0 & 0 & 0 & 1/G_{13} & 0 \\ 0 & 0 & 0 & 0 & 0 & 1/G_{12} \end{bmatrix} \quad (5)$$

The Stiffness Matrix [C] is the inverse of [S] matrix.

$$[C] = \begin{bmatrix} C_{11} & C_{12} & C_{13} & 0 & 0 & 0 \\ C_{21} & C_{22} & C_{23} & 0 & 0 & 0 \\ C_{31} & C_{32} & C_{33} & 0 & 0 & 0 \\ 0 & 0 & 0 & C_{44} & 0 & 0 \\ 0 & 0 & 0 & 0 & C_{55} & 0 \\ 0 & 0 & 0 & 0 & 0 & C_{66} \end{bmatrix} \quad (6)$$

The stiffness matrix for the transversely isotropic material is completely defined if every parameter of matrix and fiber is known and all terms inside the matrix simply depend on the aspect ratio and the volume fraction values.

2.2 Fiber Orientation Distribution function to determine the Advani-Tucker tensors

In the earliest work, to study the elastic properties of a composite taking into account the fiber orientation, each fiber was modelled as a rigid cylinder with fixed length and diameter [16]. If the fiber concentration is spatially uniform, a spherical coordinate system $\Psi(\vartheta, \varphi)$ that

represents the probability of the fiber orientation inside the unit sphere can be introduced.

Ψ is normalized and symmetric function. In addition, a vector \underline{p} describing the position of the fiber in the spherical coordinate system can be defined as follows:

$$\oint d\underline{p} = \int_{\phi=0}^{2\pi} \int_{\vartheta=0}^{\pi} \sin \vartheta d\vartheta d\phi. \quad (7)$$

The tensor Rank 2 and the tensor Rank 4 are:

$$\begin{aligned} a_{ij} &= \oint p_i p_j \Psi(\underline{p}) dp \\ a_{ijkl} &= \oint p_i p_j p_k p_l \Psi(\underline{p}) dp \end{aligned} \quad (8)$$

being $i, j, k, l = 1, 2, 3$. For a bi-dimensional material, where all fibers are located in the 1-2 plane (as it is the case for the investigated LFT), the orientation state is planar and the distribution function $\Psi_\varphi(\varphi)$ depends only on φ and the tensor Rank 2 and the tensor Rank 4 are:

$$a_{ij} = \int_0^{2\pi} p_i p_j \Psi_\varphi(\underline{p}) dp \quad (9)$$

$$a_{ijkl} = \int_0^{2\pi} p_i p_j p_k p_l \Psi_\varphi(\underline{p}) dp \quad (10)$$

Starting from the experimental data, it is not possible to describe and absolutely quantify the orientation of each fiber inside the composite, in this sense a probability distribution function to describe the spatial or plan probability distribution of the fibers is used.

2.3 Mean Tensor averaging procedure to predict the Elastic Properties of LFT

Basically, the properties of the composite are related to the probability distribution function $\Psi(\underline{p})$ and to the properties of the transversely isotropic tensor $T(\underline{p})$ by:

$$\langle T \rangle = \oint T(\underline{p}) \Psi(\underline{p}) dp \quad (11)$$

Where $\langle T \rangle$ denotes the orientation average property. The tensor $T(p_{i,j,k,l})$ is given by:

$$\begin{aligned}
T_{i,j,k,l} = & B_1(p_i p_j p_k p_l) + B_2(p_i p_j \delta_{kl} + p_k p_l \delta_{ij}) \\
& + B_3(p_i p_k \delta_{jl} + p_i p_l \delta_{jk} + p_j p_k \delta_{il}) \\
& + B_3(\delta_{ij} + \delta_{kl}) + B_5(\delta_{ik} \delta_{jl} + \delta_{il} \delta_{jk})
\end{aligned} \tag{12}$$

where δ_{ji} denotes the Kronecker delta function and the scalar B_i parameters are depending on the stiffness matrix elements (eq.6) as shown:

$$\begin{aligned}
B_1 &= C_{11} + C_{22} - 2C_{12} - 4C_{66} \\
B_2 &= C_{12} - C_{23} \\
B_3 &= C_{66} + \frac{1}{2}(C_{23} - C_{22}) \\
B_4 &= C_{23} \\
B_5 &= \frac{1}{2}(C_{22} - C_{23})
\end{aligned} \tag{13}$$

By applying the equations 12 and 13, it is possible to evaluate the elastic properties of the LFT composite weighted by the orientation distribution function. It is also important to remark that the fibers have a uniform length and constant aspect ratio (fiber length/ fiber diameter) because the volume fraction v_f is constant.

Fit functions:

3.1 Curve Fitting Procedure for FOD (Fiber Orientation Distribution)

From microstructure analysis (CT-scans) we obtain the Fiber Orientation Distribution (FOD) in terms of probability density distribution as a function of the in-plane fiber orientation for Flow and Press Regions (figure 2). As described in section 2.2, the FOD function Ψ_φ is to be symmetric and normalized. Despite different functions can be applied, not all of them satisfy the two criteria. For example, the Gaussian Function (blue curve in figure 2) is normalized and symmetric but doesn't reproduce the experimental data; on the other hand the Gauss function (Red curve) is a symmetric function suitable to fit the experimental data but it is not a normalized function. With this in mind, we selected the trigonometric function $y = \alpha + \beta \cos(x + \gamma)$ (orange curve in figure 2). The function is symmetric and normalized and it reproduces with a good agreement the experimental data, in fact it doesn't

underestimate the presence of fibers far from the 1-direction. The shape of the trigonometric function well replicates the shape of the experimental data and shows the lowest value for the quadratic error function (figure 2). The a_{ij} tensors are finally obtained by applying eq.9 and after choosing the trigonometric functions to model the Flow and the Press region. Their values

are: $\begin{pmatrix} 0.718 & -0.066 & 0 \\ -0.066 & 0.282 & 0 \\ 0 & 0 & 0 \end{pmatrix}$ and $\begin{pmatrix} 0.594 & -0.005 & 0 \\ -0.005 & 0.406 & 0 \\ 0 & 0 & 0 \end{pmatrix}$ respectively. The FOD function was used

in the computation. Therefore, we evaluate the Young's Modulus value of the composite starting from the properties of transversely isotropic material and by using the tensor procedure and the recovered FOD function. We focused on the flow region; this region is the part of the specimen where the highest degree of fiber alignment can be observed. Based on the information from section 1.3, the Halpin-Tsai theory which was developed for ideal straight fibers can most likely be applied for flow region LFT while it must be rated as critical to model press region specimens.

3.2 Curve Fitting Procedure for FLD (Fibers Length Distribution)

From specimen incineration and image analysis we can determine the Fiber Length Distribution (FLD) in terms of probability density distribution versus aspect ratio. The experimental fiber distribution as function of the aspect ratio is characterized by two main regions, see purple line in figure 3, in the first region achieved for values smaller than 500 the probability decreases strongly from 15.77% to 0.93%, in the second region scattered data are observed. For this reason, for this experimental data the distribution functions (logarithmic) used in [11] are not suitable. Our investigations indicate as more appropriate curves the ones shown in figure 3: (i) the exponential function (the red curve: $y = e^{a+bx}$) and (ii) the hyperbolic function (the orange curve $y = a/x$). The experimental range of the aspect ratio is between 27 and 3340. We can observe that: both red and orange curves in figure 3 are in good

agreement to the experimental data for low values of aspect ratio (smaller than 200); the percentage amount of the fibers with aspect ratio less than 200 is 37.24% and 50.18% respectively. In particular, the 32.8% of the fibers have an aspect ratio values smaller than 120 and the 15.77% of the fibers have aspect ratio equal to 27. For higher values of aspect ratios scattered data are observed. In this condition, two main mistakes could be occur, (i) to underestimate the E_{11} value if we focus on the lower aspect ratio or (ii) to exclude a high amount of fibers if we focus on the higher aspect ratio values..Furthermore the orange curve follows well the experimental data for high values of aspect ratio. All curves are fitted with data inside the experimental range of AR. Outside this range, it doesn't make sense to recover the FLD, because values lower than 27 correspond to fiber fragments with low load-carrying ability and values higher than 2500 are less relevant for our investigation as the elastic stiffness has almost reached its saturation level for AR above 1000.

Results obtained by using the recovered functions for FOD and FLD and by using the Mean Tensor Averaging Procedure

The last part of this work is related to the prediction of the properties of LFT through the combination of the Halpin Tsai theory, the orientation distribution function, the mean tensor averaging procedure and the length distribution function.

- The **first** step is to evaluate the elastic properties of the transversely isotropic material from the Halpin-Tsai theory. As known, for a fixed fiber volume fraction, the elastic stiffness of the transversely isotropic composite in the 1 direction (E_{11}) is expressed as function of the aspect ratio and its value increases highly for low values of aspect ratio and up aspect ratio equal to 200 reaches a constant value near. This behaviour is independent on the value of fiber volume fraction. To achieve the curves we used for fibers and matrix the data shown in the appendix (table a) under application of equations from eq.1 to eq.4.

- The **second** step is to apply the mean tensor averaging procedure to take into account the orientation distribution function. The Elastic Modulus of the composite is evaluated by using the eq.11 and the FOD identified from experimental data. As shown in figure 4 for volume fraction values between 13% and 18%, E_{11} depends on the aspect ratio up to 200, for larger values the modulus does not change appreciably. In the figure 4, the purple points are the constant experimental value (see section 1.1). From this point of view, it seems that the composite with similar mechanical properties has a volume fraction between 17% and 18%, which is well above the nominal value of 13% of the investigated material. However, to have a full overview about the elastic modulus we have to take into account the amount of each fiber inside the composite that means that we have to weigh the Elastic modulus values on the FLD.

- The **third** step is to use the recovered fit function to achieve the experimental distribution lengths data, for weighting the E_{11} obtained from the previous Tensor procedure.

A recovered fit function for each E_{11} values is found. As an example, figure 5 shows for $v_f=13\%$, the E_{11} value for the following cases: (i) a perfect fiber aligned (in 1-direction) composite (**thick blue line**) computed by using Halpin-Tsai equations; (ii) the Tensor procedure explained in the second step (**dashed blue line**) computed by using the tensor procedure; and (iii) the recovered distribution function of the previous function (**continuous blue line**).

Applying the procedure we obtain the E_{11} value for each volume fraction value as indicated in table b. By using this procedure it is possible to evaluate the E_{11} value for a fixed volume fraction with the experimental distribution length function. For $v_f=13.29\%$ the $E_{11}=8.70\text{GPa}$.

Conclusion

A hybrid methodology to predict the Young's modulus of a Long Fiber Thermoplastic composite was developed in detail in this paper. Experimental data for fiber length

distribution and for orientation distribution was used to obtain the fitting functions and to combine the fitting functions with the Halpin Tsai equations. Our results indicate that our approach can be used with success to predict the stiffness value for a fixed volume fraction, and to estimate the volume fraction using a fixed stiffness value. We conclude that: a) if we don't take into account the experimental length distribution we overrate the volume fraction; b) to improve the good agreement with the experimental results, we need more accurate experimental data for FLD; c) if our threshold is the experimental value of stiffness (7.83 GPa) the obtained volume fraction assumes a lower value than the expected one (11.5%). To reach the point b), we need to take into account a larger amount of fibers, in our case it is around 50% between the AR range ($27 < AR < 1000$); for higher AR values, experimental measurements show scattered data so we need more experimental investigations for improving this point. This could also explain the point c): the detected volume fraction value is lower than the experimental one because if we used only the 50% of the total amount of the real fiber present in the specimen we underestimate the presence of the fiber inside the composite. We focus on predicting the young's modulus of LFT by using, as much as possible, the experimental data in terms of DOF and FLD. if we compared the value obtained with the experimental one, we can say that the proposed methodology can be considered useful for the purposes of the prediction of Young's modulus.

References

- [1] Charles L. Tucker III, Erwin Liang - *Stiffness predictions for unidirectional short-fiber composites: Review and evaluation* - Composites Science and Technology 59 (1999) pp655-667.
- [2] J. C. Halpin, J. L. Kardos - *The Halpin-Tsai Equations: A Review* - Polymer Engineering and Science 16-5 (1976) 344-352

- [3] Peter J. Hine, Hans Rudolf Lusti, Andrei A. Gusev - *Numerical simulation of the effects of volume fraction, aspect ratio and fiber length distribution on the elastic and thermoelastic properties of short fiber composites*- - Composites Science and Technology 62 (2002) 1445–1453.
- [4] Peter J. Hine, Hans Rudolf Lusti, Andrei A. Gusev - *On the possibility of reduced variable predictions for the thermoelastic properties of short fibre composite*- Composites Science and Technology 64 (2004) 1081-1088
- [5] Hans Rudolf Lusti, Peter J. Hine, Andrei A. Gusev - *Direct numerical predictions for the elastic and thermoelastic properties of short fibre composites* - Composites Science and Technology 62 (2002) 1927–1934
- [6] Delphine Dray, Pierre Gilormini, Gilles Régnier – *Comparison of several closure approximations for evaluating the thermoelastic properties of an injection molded short-fiber composite* – Composite Science and Technology 67 (2007) 1601-1610
- [7] Babatunde O. Agboola, David A. Jack, Stephen Montgomery-Smith - *Effectiveness of recent fiber-interaction diffusion models for orientation and the part stiffness predictions in injection molded short-fiber reinforced composites* - Composites: Part A vol 43 (2012) 1959–1970
- [8] Doo Jin Lee, Hwajin Oh, Young Seok Song, Jae Ryoung Youn– *Analysis of effective elastic modulus for multiphased hybrid composite* – Composite Science and technology 72 (2012) 278-283.
- [9] H.L. Duan, X. Yi, Z.P. Huang, J. Wang - *A unified scheme for prediction of effective moduli of multiphase composites with interface effects. Part I: Theoretical framework* - Mechanics of Materials 39 (2007) 81–93

- [10] H.L. Duan, X. Yi, Z.P. Huang, J. Wang - *A unified scheme for prediction of effective moduli of multiphase composites with interface effects: Part II—Application and scaling laws* - Mechanics of Materials 39 (2007) 94–103
- [11] Chin, W.K., Liu, H.T. and Lee, Y.D - *Effect of Fiber Length and Orientation Distribution on the Elastic Modulus of Short Fiber Reinforced Thermoplastics*, Polymer Composites, 9: (1988). 27–35.
- [12] Nguyen, BN, Bapanapalli, SK, Holbery, JD, Smith MT, Kunc, V, Frame, BJ, Phelps, JH, Tucker, CL - *Fiber length and orientation in long-fiber injection-molded thermoplastics - Part I: Modeling of microstructure and elastic properties* – Journal of Composite Materials 42-10 (2008) 1003-1029 DOI: 10.1177/0021998308088606
- [13] Y. P. Qiu and G. J. Weng – *On the application of Mori-Tanaka's theory involving transversely isotropic spheroidal inclusions*- International Journal EngngSci. (1990) Vol. 28, No. 11, pp. 1121-1137.
- [14] S.I. Kundalwal, M.C. Ray - *Effective properties of a novel composite reinforced with short carbon fibers and radially aligned carbon nanotubes*- Mechanics of Materials vol. 53 (2012) 47–60
- [15] Jia-Lin Tsai, Shi-Hua Tzeng, Yu-Tsung Chiu - *Characterizing elastic properties of carbon nanotubes/polyimide nanocomposites using multi-scale simulation* - Composites: Part B vol.41 (2010) 106–115
- [16] S.G. Advani, C.L. Tucker III – *The use of tensors to describe and predict fiber orientation in short fiber composites*- Journal of Rheology, 31 (1987) 751–784.
- [17] Hoehn, N., *FASEP® fiber separation and length determination procedure*, <http://www.fasep.de>, 2013-03-06

- [18] Troester, S., *Materialentwicklung und –charakterisierung fuer thermoplastische Faserverbundwerkstoffe im Direktverfahren, Dissertation*, University of Stuttgart, Germany, 2003
- [19] Seelig, T., Latz, A., Sanwald, S., *Modelling and crash simulation of long-fibre-reinforced thermoplastics*, 7. LS-DYNA Anwenderforum, Bamberg, Germany, 2008
- [20] Tinevez, J.: *Directionality plugin for ImageJ*, <http://fiji.sc/wiki/index.php/Directionality>, 2013-03-06
- [21] Gusev, A; Lusti, HR; Hine, PJ - *Stiffness and thermal expansion of short fiber composites with fully aligned fibers* – *Advance Engineering Materials* 4 12 (2002) 927-931 - DOI: 10.1002/adem.200290007
- [22] Gusev, A; Heggli, M; Lusti, HR; et al. - *Orientation averaging for stiffness and thermal expansion of short fiber composites* - *Advance Engineering Materials* 4 12 (2002) 931-933 - DOI: 10.1002/adem.200290008

Figures and Tables

E_f	72,00	[GPa]	Fiber Young's Modulus
ν_f	0,22		Fiber Poisson's ratio
d_f	0.017	[mm]	Fiber diameter
E_m	1,40	[GPa]	Matrix Young's Modulus
ν_m	0,35		Matrix Poisson's ratio
Table a – Fiber (f) and matrix (m) properties			

Volume Fraction	E_{11} [GPa]
12%	8.06
13%	8.54
14%	9.05
15%	9.56
16%	10.05
17%	10.58
18%	11.09
Table b - Analytically predicted E_{11} values for flow region LFT at different volume fraction values	

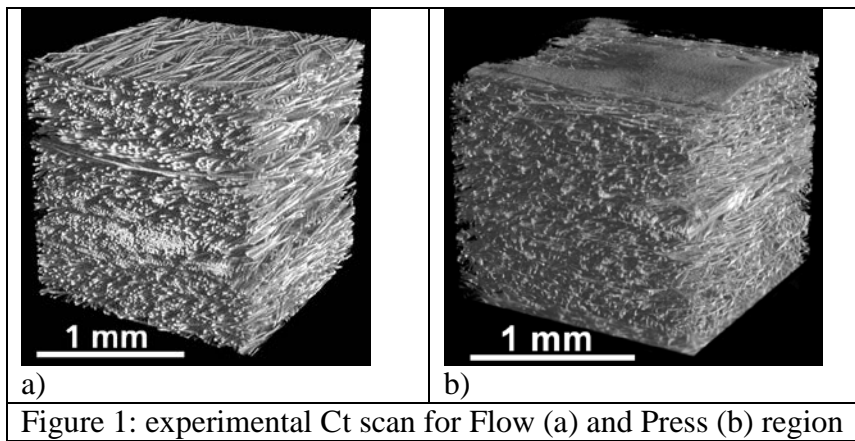


Figure 1: experimental Ct scan for Flow (a) and Press (b) region

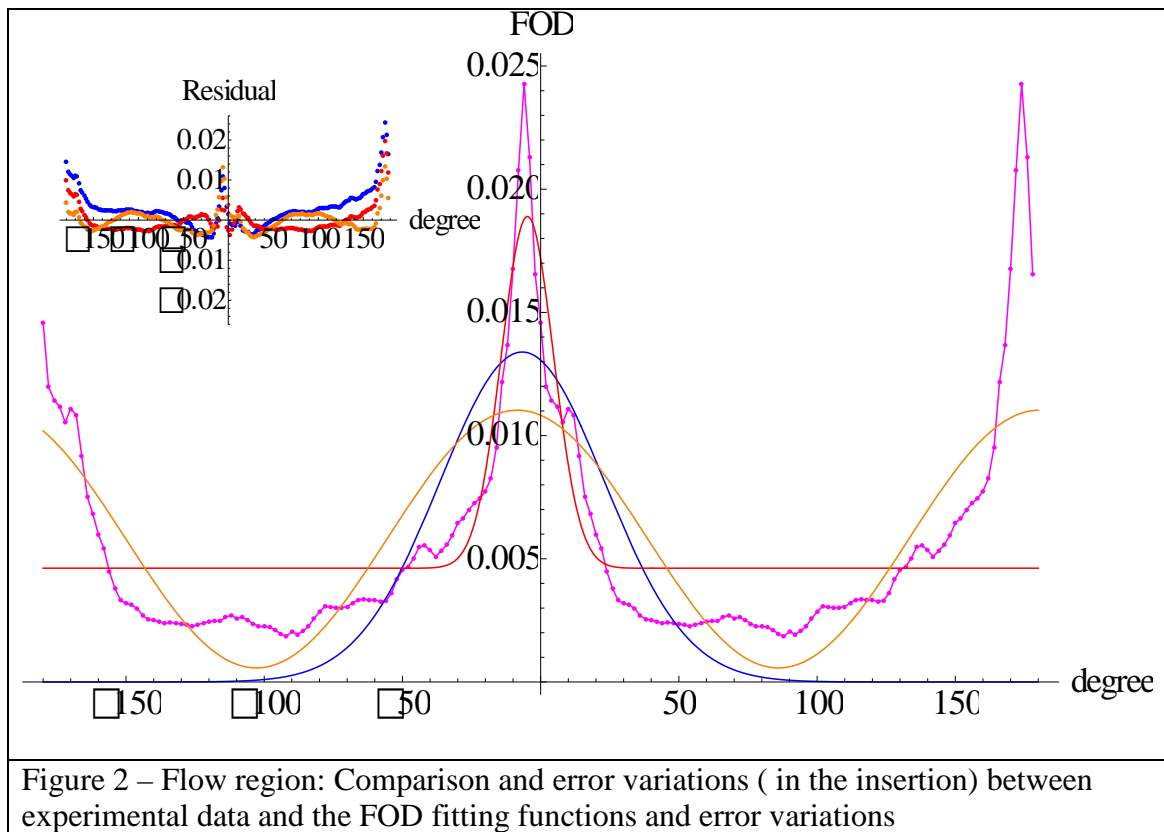
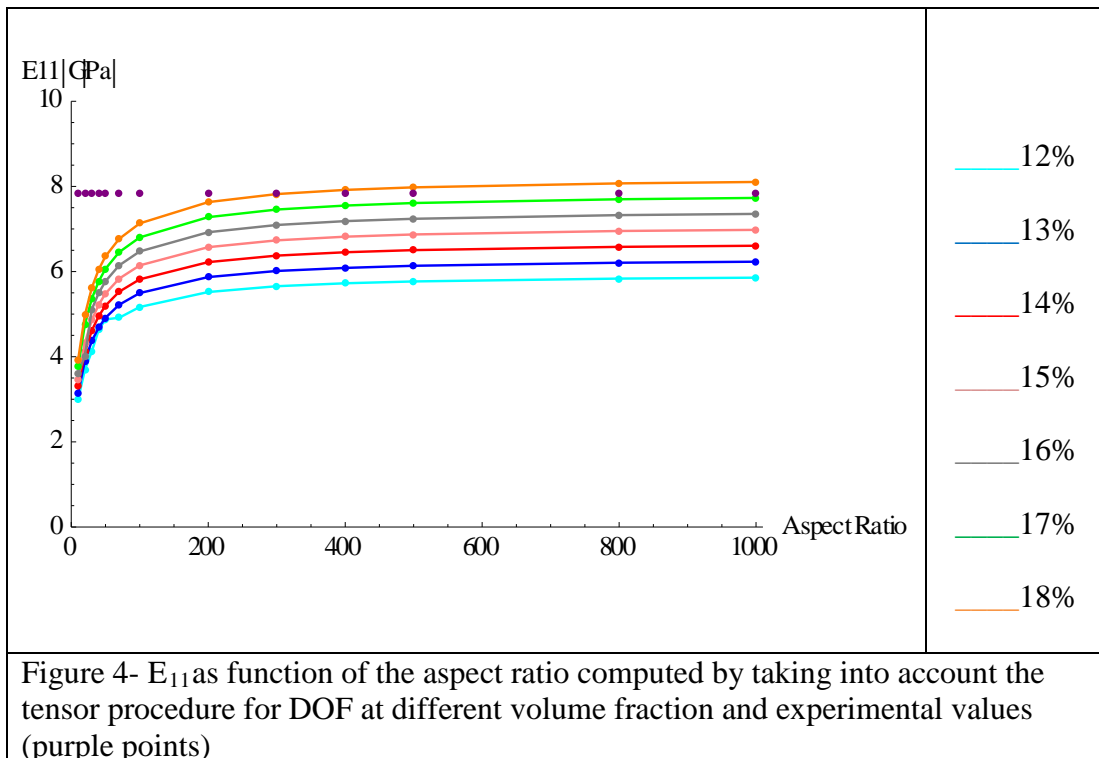
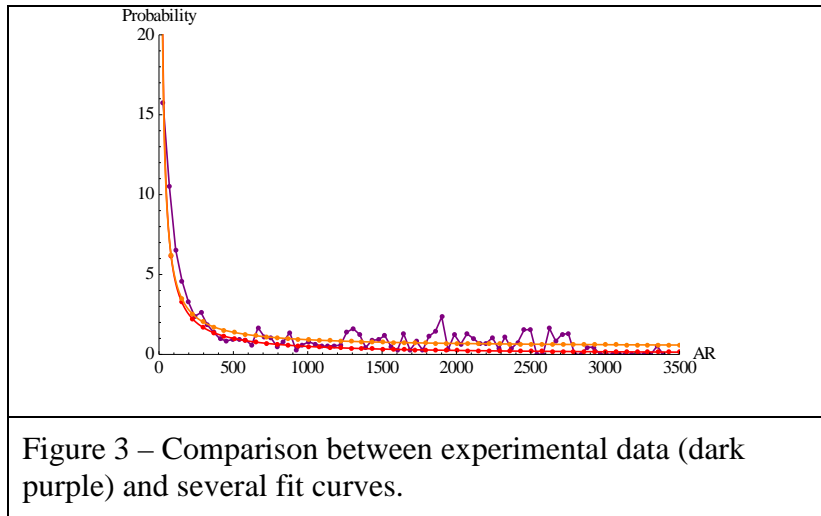


Figure 2 – Flow region: Comparison and error variations (in the insertion) between experimental data and the FOD fitting functions and error variations



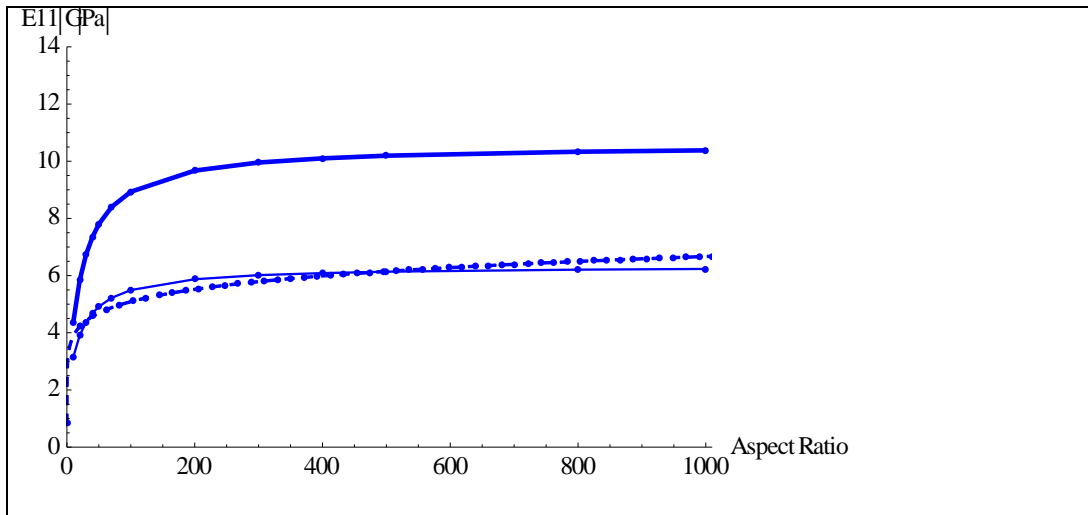


Figure 5 – E_{11} as function of the aspect ratio achieved for a transversely isotropic material (thick blue line), by using tensor procedure (dashed line) and by using the recovered fit function (continuous line) for a fixed volume fraction value (13%)